Available online at www.sciencedirect.com
SCIENCE DIRECT®
Journal of Power Sources 154 (2006) 202–213
JOURNAL OF POWER SOURCES
www.elsevier.com/locate/jpowsour

Review

Architecture for portable direct liquid fuel cells

Weimin Qian [a,b], David P. Wilkinson [a,b,*], Jun Shen [a], Haijiang Wang [a], Jiujun Zhang [a]

[a] *Institute for Fuel Cell Innovation, National Research Council, 3250 East Mall, Vancouver, BC, Canada V6T 1W5*
[b] *Department of Chemical and Biological Engineering, The University of British Columbia, 2216 Main Mall, Vancouver, BC, Canada V6T 1Z4*

Received 30 November 2005; accepted 15 December 2005
Available online 19 January 2006

Abstract

Direct fuel cells (DFCs) are receiving increased interest for portable power applications. Cell and stack architecture is a vital technical issue for portable DFCs. The architecture of a DFC not only has to meet particular application requirements such as a compact size and easy handling, but also has to ensure desired performance, reliability and fabrication costs. In this paper, the most recent advances related to portable DFCs and their architecture are reviewed. The current status of system architecture, stack/unit cell architecture, flow-field designs and MEA morphology strategies along with analysis are surveyed. In addition, promising methods of passive fuel delivery are also presented.

Keywords: Direct fuel cell; Architecture; Passive; Bi-cell; Flow field; MEA morphology

Contents

* Corresponding author. Tel.: +1 604 822 4888; fax: +1 604 822 6003.
E-mail address: dwilkinson@chml.ubc.ca (D.P. Wilkinson).

0378-7753/$ – see front matter © 2005 Elsevier B.V. All rights reserved.
doi:10.1016/j.jpowsour.2005.12.019

1. Introduction to portable DFCs

Within the last 10 years, there has been an increased interest in direct fuel cells (DFCs), particularly in the area of polymer electrolyte membrane (PEM) fuel cells. DFCs use liquid fuels (in liquid or vapor form) directly as a fuel without a reforming step. The most commonly used liquid fuels in direct fuel cells include methanol, ethanol, formic acid, etc. Although hydrogen can be used as a direct fuel, these liquid fuels usually have much higher volumetric energy density. Moreover, these liquid fuels are much easier to store, transport and refill. Therefore, DFCs usually have a compact design and potentially can offer up to 10 times the energy density of rechargeable batteries. In addition, DFCs can be designed to operate at ambient temperature, which significantly reduces thermal management challenges for small systems. These advantages make the technology attractive to the rapid growing need for portable power sources from the sub-Watt range up to a few hundred Watts. For clarification, in accordance with the literature, portable DFCs should include micro- and small DFCs.

Although not an issue with hydrogen fuel cells, DFCs have to deal with issues such as the sluggish anode kinetics and fuel crossover. The slow anode kinetics comes from a multi-step fuel oxidation process at the anode, and this results in higher anodic overpotentials. The fuel crossover from anode to cathode through a polymer electrolyte membrane is another major cause of power losses in DFCs. The crossover not only lowers the fuel utilization, but also degrades the cathode performance and generates extra heat. Other issues such as anode gaseous product removal and water recovery may also add extra complications to the DFC.

Among different fuel candidates, methanol shows good electrochemical activity with a high energy density, and it can be generated from a number of different sources like natural gas, coal, or biomass. Therefore, direct methanol fuel cells (DMFCs) have received the most extensive attention and efforts compared to other types of DFCs. Significant improvements have been made in the performance of the DMFC. However, DMFCs still have some significant issues such as low activity of the state-of-the-art electrocatalysts and methanol cross-over as the critical barriers to their commercialization. In addition, methanol as a fuel is relative toxic and requires adequate safety precautions.

Ethanol is a promising alternative fuel choice due to its higher energy density, non-toxicity, and availability from renewable energy sources. It can be easily produced in large quantity using sugar-containing raw materials from agriculture or biomass. Although the complete electro-oxidation of ethanol to CO_2 involves carbon-carbon bond rupture, previous studies have shown that the electrochemical reactivity of ethanol over Pt-based catalysts is not significantly lower than that of methanol. Ethanol also shows a lower permeability/crossover rate and it has a less serious effect on the cathode performance than methanol [1].

Formic acid as a fuel has gained special interest in recent years. One of the biggest advantages with formic acid is its much lower crossover rate through a Nafion® membrane than that of methanol. The crossover of formic acid has shown a reduction by "two orders of magnitude" compared with methanol [2]. Moreover, very recent research reported that Pd has superior catalytic behavior for electro-oxidation of formic acid [3]. With this Pd catalyst, the direct formic acid fuel cell has generated very promising power densities of 255–230 mW cm^{-2} at relatively high voltages of 0.40–0.50 V over a wide range of formic acid concentrations from 3.0 to 15.0 M, and with dry ambient air supplied at a room temperature of 20 °C. These performances are much higher than a direct methanol fuel cell (DMFC) with power density of 50 mW cm^{-2}, under comparable conditions. In addition, formic acid is generally safe and non-toxic. These promising direct formic acid fuel cells (DFAFCs) are likely to become one of the first commercial small fuel cell power sources on the market. With respect to drawbacks, formic acid is currently more expensive than methanol and its energy density is lower (about one-third of pure methanol).

In addition, other liquid chemicals have also been investigated as fuels for different DFCs, such as 2-propanol [4,5], dimethyl ether (DME) [6], ethylene glycol (EG) [7], dimethoxymethane (DMM) [8,9], trimethoxymethane (TMM) [9,10], tetramethyl orthocarbonate (TMOC) [11] and hydrazine [12,13]. Table 1 provides a comparison of the reactions, cell potentials, energy densities, theoretical efficiency and other selected properties for different fuels.

As researchers try to develop promising DFCs using various fuels and corresponding catalyst materials, architecture is always a vital technical issue. The architecture of a DFC not only has to meet particular application requirements such as a compact size and ease of handling, but also has to ensure desired performance, reliability and fabrication costs.

The goal of this paper is to review the most recent advances related to the architecture of portable DFCs. Since a DFC device is a complex system, its architecture also has different corresponding levels of complexity, i.e. from the top overall system level down to the microstructure level of a component (e.g. MEA). Taking a top down approach, system architecture will be reviewed first followed by stack/unit cell architecture and flow field design. Lastly, more detailed strategies along with analysis of MEA architecture are presented. In addition, promising methods of passive fuel delivery are addressed. The general approach in this paper is to outline the issues and problems followed by approaches with examples.

2. Current status of architecture for DFCs

2.1. System architecture

In this paper, system architecture of a DFC is considered to be the sum of all the components with their structure and layout based on the reactants supply and operation mode to deliver a required power output.

2.1.1. Active versus passive fuel/oxidant supply

There exist two types of systems: "active" and "passive". Active systems use extra balance-of-plant components such as a pump and a fan for cooling, humidification, reactant and product control as shown in Fig. 1 [14]. With these additional compo-

Table 1
Possible fuels for DFCs with reaction equations and selected properties[a]

Fuels	Reactions		$-\Delta G^0$ (kJ mol^{-1})	Standard theoretical potential, E^0	Energy density (Wh L^{-1})	$-\Delta H^0$ (kJ mol^{-1})	Reversible energy efficiency
Hydrogen	Anode	$H_2 \rightarrow 2H^+ + 2e^-$	0	0.000 V			
	Cathode	$2H^+ + 2e^- + (1/2)O_2 \rightarrow H_2O_{(l)}$		1.229 V			
	Overall	$H_2 + (1/2)O_2 \rightarrow H_2O$	237.1	1.229 V	180 (@ 1000 psi, 25 °C)	285.8	0.830
Methanol	Anode	$CH_3OH_{(l)} + H_2O \rightarrow CO_2 + 6H^+ + 6e^-$	9.3	0.016 V			
	Cathode	$6H^+ + 6e^- + (3/2)O_2 \rightarrow 3H_2O_{(l)}$		1.229 V			
	Overall	$CH_3OH_{(l)} + (3/2)O_2 \rightarrow CO_2 + 2H_2O_{(l)}$	702	1.213 V	4820 (100 wt.%)	726	0.967
Ethanol	Anode	$C_2H_5OH_{(l)} + 3H_2O \rightarrow 2CO_2 + 12H^+ + 12e^-$	97.3	0.084 V			
	Cathode	$12H^+ + 12e^- + 3O_2 \rightarrow 6H_2O_{(l)}$		1.229 V			
	Overall	$C_2H_5OH_{(l)} + 3O_2 \rightarrow 2CO_2 + 3H_2O_{(l)}$	1325	1.145 V	6280 (100 wt.%)	1367	0.969
Formic acid	Anode	$HCOOH_{(l)} \rightarrow CO_2 + 2H^+ + 2e^-$	−33	−0.171 V			
	Cathode	$2H^+ + 2e^- + (1/2)O_2 \rightarrow H_2O_{(l)}$		1.229 V			
	Overall	$HCOOH_{(l)} + (1/2)O_2 \rightarrow CO_2 + H_2O_{(l)}$	270	1.400 V	1750 (88 wt.%)	254.3	1.062
2-Propanol	Anode	$C_3H_7OH_{(l)} + 5H_2O \rightarrow 3CO_2 + 18H^+ + 18e^-$	186.3	0.107 V			
	Cathode	$18H^+ + 18e^- + (9/2)O_2 \rightarrow 9H_2O_{(l)}$		1.229 V			
	Overall	$C_3H_7OH_{(l)} + (9/2)O_2 \rightarrow 3CO_2 + 4H_2O_{(l)}$	1948	1.122 V	7080 (100 wt.%)	2005.6	0.971
Hydrazine	Anode	$N_2H_{4(l)} \rightarrow N_2 + 4H^+ + 4e^-$	−149.2	−0.386 V			
	Cathode	$4H^+ + 4e^- + O_2 \rightarrow 2H_2O_{(l)}$		1.229 V			
	Overall	$N_2H_{4\ (l)} + O_2 \rightarrow N_2 + 2H_2O_{(l)}$	623.4	1.615 V	5400 (100 wt.%)	622.2	1.002
Dimethyl ether (DME)	Anode	$(CH_3)_2O_{(g)} + 3H_2O \rightarrow 2CO_2 + 12H^+ + 12e^-$	35.4	0.031 V			
	Cathode	$12H^+ + 12e^- + 3O_2 \rightarrow 6H_2O_{(l)}$		1.229 V			
	Overall	$(CH_3)_2O_{(g)} + 3O_2 \rightarrow 2CO_2 + 3H_2O_{(l)}$	1387.2	1.198 V	5610 (in liquid of 100 wt.%)	1460.3	0.950
Ethylene glycol (EG)	Anode	$C_2H_6O_{2(l)} + 2H_2O \rightarrow 2CO_2 + 10H^+ + 10e^-$	8.78	0.009 V			
	Cathode	$10H^+ + 10e^- + 5/2O_2 \rightarrow 5H_2O_{(l)}$		1.229 V			
	Overall	$C_2H_6O_{2(l)} + 5/2O_2 \rightarrow 2CO_2 + 3H_2O_{(l)}$	1176.7	1.220 V	5870 (100 wt.%)	1189.5	0.990
Dimethoxymethane (DMM)	Anode	$(CH_3O)_2CH_{2(l)} + 4H_2O \rightarrow 3CO_2 + 16H^+ + 16e^-$	2.18	0.002 V			
	Cathode	$16H^+ + 16e^- + 4O_2 \rightarrow 8H_2O_{(l)}$		1.229 V			
	Overall	$(CH_3O)_2CH_{2(l)} + 4O_2 \rightarrow 3CO_2 + 4H_2O_{(l)}$	1894.6	1.227 V	5970 (100 wt.%)	1937.5	0.978
Trimethoxymethane (TMM)	Anode	$(CH_3O)_3CH_{(l)} + 5H_2O \rightarrow 4CO_2 + 20H^+ + 20e^-$	–[b]	–			
Tetramethyl orthocarbonate (TMOC)	Anode	$(CH_3O)_4C_{(l)} + 6H_2O \rightarrow 5CO_2 + 24H^+ + 24e^-$	–	–			

[a] Under standard condition (25 °C, 1 atm) unless specified.
[b] No thermodynamic data available from sources to author's knowledge.

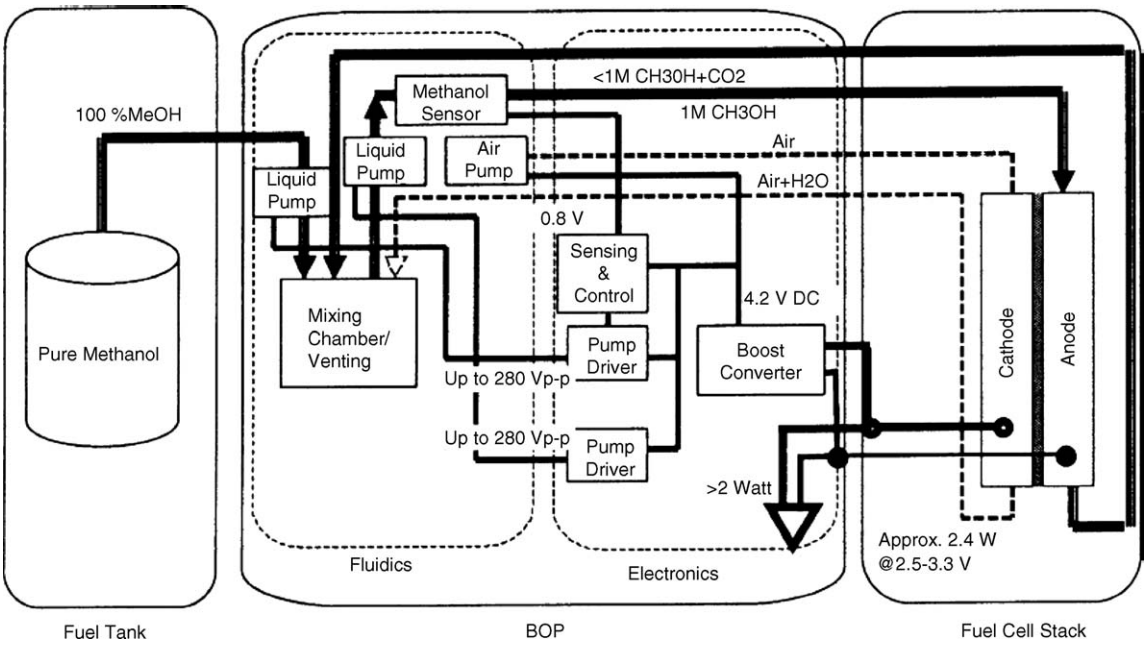

Fig. 1. A schematic diagram of a low power direct methanol fuel cell (DMFC) active system [14], ©(2004), with permission from Elsevier.

nents in the system, active systems can be operated at favourable conditions with respect to temperature, pressure, concentration and flow rate. This will improve fluid mass transport and electrochemical activity. Therefore, higher current density and output power can be achieved, but at the cost of greater system complexity and lower system energy density. In general, active systems are better suited for larger fuel cells.

Passive systems only use natural capillary forces, diffusion, convection (air breathing) and evaporation to achieve all processes without any additional power consumption. They are usually operated at low current density resulting in reduced cooling load, less water management issues, less heat production and a lower required fuel delivery rate [15]. Therefore, by using a well-designed compact architecture, a passive system can achieve higher reliability, lower cost, higher fuel utilization and maximum system energy density, making it more suitable for portable power sources.

The world's smallest new DMFC from Toshiba shown in Fig. 2 adopts a "passive" fuel supply system, which feeds a highly concentrated methanol fuel solution (99.5%) directly into the cell [16]. The company has optimized the structure of the fuel cell's electrodes and polymer electrolyte membrane to address the crossover problem. A very high energy density (270 Wh L^{-1}) is achieved.

2.1.2. Vapor-feed versus liquid-feed systems

Some earlier research [17,18] showed that the performance of vapor-feed DMFCs could achieve a significant improvement in performance over that reported for the liquid-feed DMFC. However, there has only been limited report on vapor-feed systems, recently. This is largely due to the complexity of the vapor-feed systems, which are presently not preferred for the application of portable power sources. Some pros and corns for both types of systems are listed in Table 2.

2.2. Unit cell and stack architecture

2.2.1. Unit cell configurations

In a fuel cell stack, the basic unit cell can be configured as a unit single cell or a unit bi-cell as shown in Fig. 3. In a unit single cell arrangement (Fig. 3a), fluid flow field plates are placed on each side of a membrane electrode assembly (MEA) to form the anode and the cathode compartments. The plates provide channels for the access of reactants and removal of gas product and water formed during operation of the cell to/from the respective anode and cathode. These plates also act as current collectors.

In a unit bi-cell arrangement (Fig. 3b), two cells are placed with their anodes spaced apart and facing each other. The spacer also serves as the fuel distributor and the current collector. With this layout, fuel is distributed to the sealed anode space by either active or passive means. On the other hand, ambient air is easily accessed from the outside-facing cathodes.

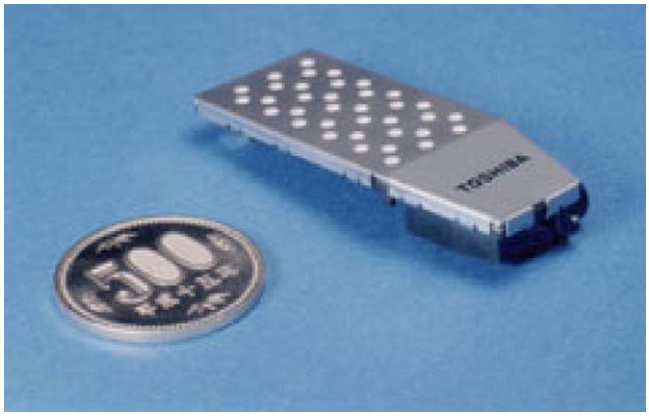

Fig. 2. The world's smallest new DMFC from Toshiba, courtesy of [16].

Table 2
Comparison of vapor-feed vs. liquid-feed DFC systems

System	Advantage	Disadvantages
Liquid-feed DMFC	Simpler system More compact in size and weight No need for separate cooling system (when in active operation mode) No need for separate humidification system (simple membrane hydration) Suitable for portable applications	Needs dilution of liquid fuels at anode Maximum operating temperature <90 °C Limiting two-phase mass transfer at both anode and cathode Lower electrochemical activity and performance Requires liquid diffusion electrodes
Vapor-feed DMFC	Better performance with: Favorable faster single-phase anode mass transfer and less crossover Enhanced anode kinetics at higher operating temperatures and pressures Can use concentrated fuels Can use conventional gas diffusion electrodes	More complex system with controls, e.g. in pressure and temperature Larger and heavier system Needs separate cooling system Needs separate membrane humidification

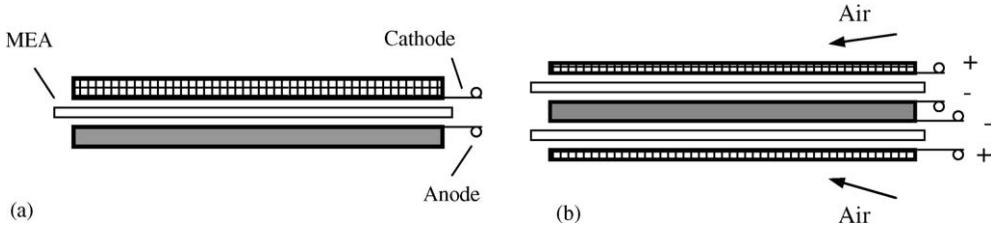

Fig. 3. Unit cell configurations: (a) unit single cell; (b) unit bi-cell.

2.2.2. *Stack configurations*

(1) Bipolar stack: Two or more unit cells are often in contact and connected together to form a stack. Unit single cells are typically aligned face to face to form a serial stack to provide higher output voltage as shown in Fig. 4a. In this arrangement, the adjacent anode and cathode flow field plates are usually made into one plate called the bipolar plate. The stack typically includes manifolds, inlets and outlets for directing pressurized fuels and oxidants to and from the anode and cathode, respectively, in the flow field channels. In DFC applications, separate coolant and humidification circuits are usually eliminated since the forced liquid fuel flow can also serve the cooling function and in some cases provide humidification. Obviously, this type of stack is suitable for those active DFC systems.

(2) Bi-cell stack: Unit bi-cells can be formed into a stack as shown in Fig. 4b. In this arrangement, an appropriate gap is made between bi-cell units to allow adequate air access. Heat and water can also be removed by natural or forced convection. A unique feature for this arrangement is the possibility of identifying and replacing a particular defective bi-cell unit without disassembling or disrupting the operation of the entire stack.

(3) Mono-polar strip stack: In this special arrangement, unit single cells are placed side by side to form a mono-polar strip stack [19,20] as shown in Fig. 4c. In this case, air can be supplied to one side of the stack by spontaneous convection. There is no need for an air pump or blower. Liquid fuel can be accessed by either active distribution with flow field channels, or by passive distribution.

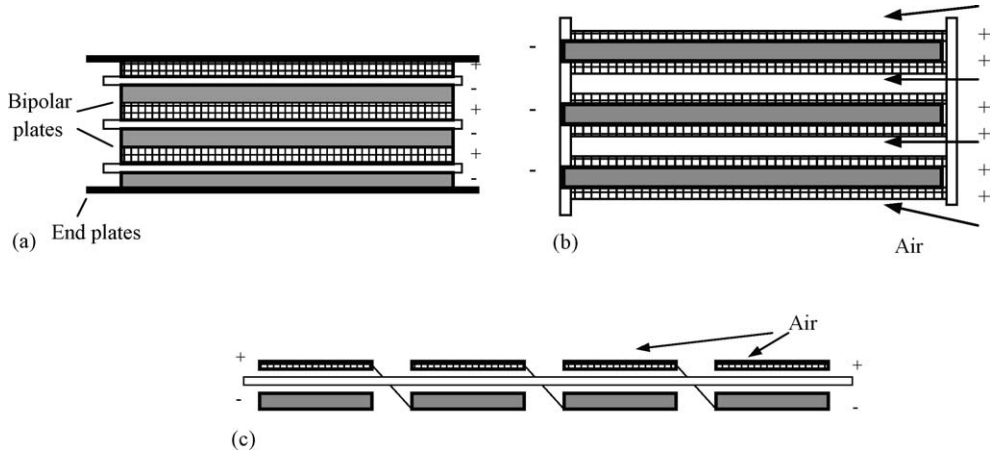

Fig. 4. Stack configurations: (a) bipolar parallel; (b) bi-cell parallel; (c) mono-polar strip.

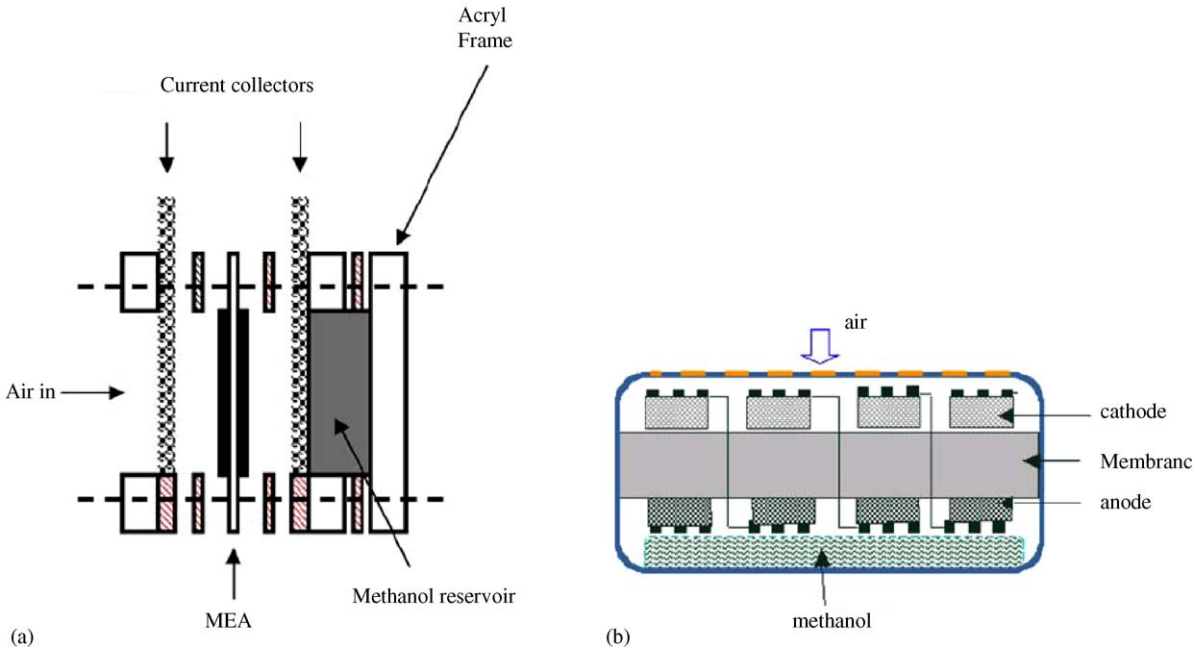

Fig. 5. Passive air breathing DMFC examples: (a) a passive type DMFC cell [21]; (b) a passive type DMFC stack [22], ©(2004), with permission from Elsevier.

Passive stack systems show many unique features, and are attracting more interest for portable power sources. Examples of passive air breathing DMFC cells are shown in Fig. 5 [21,22]. Examples of bi-cell units are shown in Fig. 6 [23,24] and show some promising performance and advantages. Many of these cell configurations have not been tested in practical applications yet.

2.3. Flow field design

In terms of functionality, the main tasks of flow-field plates are to act as current-collectors, provide mechanical support, keep reactants separate and to allow distribution of reactants and removal of products over the reaction surface area. Flow-field design and method of operation highly influence the perfor-

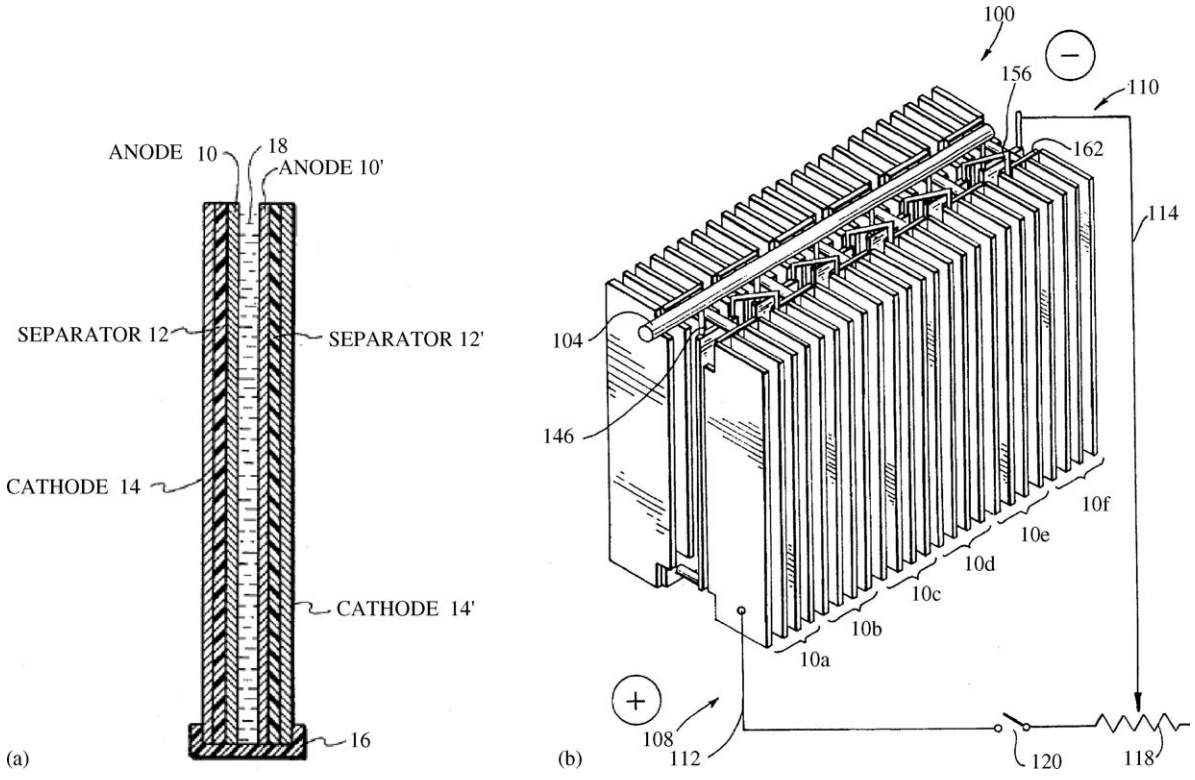

Fig. 6. Examples of bi-cell units: (a) a bi-cell unit for a hydrazine-air fuel cell [23]; (b) a bi-cell stack for a hydrogen-air fuel cell [24].

mance and stability of active DFCs. The bipolar plates can account for 12–8% of the total fuel-cell-stack cost, more than 80% of the stack weight, and nearly all the stack volume [25]. Therefore, improvements in the bipolar plate can significantly improve stack performance, and reduce stack weight, size and cost.

2.3.1. Flow field configurations

Different types of flow fields for DFCs have been presented in the literature [26–32]. They are, namely, straight (parallel), serpentine (meander), spot (pin or grid), and interdigitated channels as shown in Fig. 7. A comparison of these different flow fields is given in Table 3.

In general, different flow field designs have pros and cons associated with their application. Proper selection of flow fields and fine-tuning of the dimensional designs with respect to the DFCs' operational and application conditions can help achieve cost and performance goals. Serpentine and parallel channel flow fields are the most commonly used for active DFCs. In passive DFC systems without flow fields, the porous diffusion media is critical to reactant distribution and performance.

2.3.2. Stack reactant feed configurations

In a DFC stack, the method of reactant distribution to the individual cells is also of great importance. Liquid fuels or air can be fed either in series or in parallel, as shown in Fig. 8. The serial configuration forces a reactant feed and product removal flow stream from one cell to another in series. Higher pressure-drop occurs as a result of the longer traveling length for the stream. The reactant distribution is normally not uniform from cell to cell along the reactant feed path. But the continuous flow without any bypass is beneficial for product gas and water removal. The parallel configuration has lower pressure-drop, but can result in non-uniform reactant distribution flow between cells due to uneven product gas bubbles and water droplets formed in the channels of each of the cells. In the worst case, non-uniform cell-to-cell reactant distribution can lead to low cells and cell reversal.

2.4. Membrane electrode assembly (MEA) design

The MEA is the most important and critical component of the direct liquid fuel cell. It faces more challenges than the standard PEMFC due to the slow anode kinetics, two-phase mass transport at the anode, and fuel and water crossover to the cathode. MEA design for the DFC should seek to incorporate: (i) membranes with low fuel permeability; (ii) anodes with improved catalysts; (iii) anode structure to enhance two-phase mass transport and catalyst utilization; (iv) selective cathode catalysts that are insensitive to fuel crossover; and (v) cathode catalyst layer structures that are less susceptible to water flooding due to the reaction and crossover from the anode. To be consistent with the focus of this paper, only the structural aspects of the MEA design will be discussed.

2.4.1. Different MEA configurations with respect to the DFC

Three types (A, B and C) of MEA configuration for DFCs are presented in Fig. 9 [33]. The type A MEA uses the common approach, which starts with spaying the microporous diffusion layer on to a carbon cloth backing followed by a catalytic layer sprayed on top. The MEA is assembled by hot-pressing the catalytic coated backings on a pre-treated Nafion® membrane. For the type B MEA, the catalytic ink is sprayed directly onto the membrane. The catalyst-coated membrane (CCM) is then combined with two diffusion backings by hot pressing. For the type C MEA, the microporous diffusion layer is prepared by applying the carbon ink on the catalyst-coated membrane (CCM) instead of the carbon cloth. The carbon cloth is finally attached by hot-pressing. Comparatively, the type C MEA achieved the best results due to the enhanced quality of contact between the catalyst layer, microporous diffusion layer and the membrane. Nordlund et al. [34] and Song et al. [35] have also addressed the importance of the quality of contact between the catalyst layer and the membrane to the catalyst loading efficiency and overall MEA performance. As an alternative approach, catalyst-coated membranes (CCM) was fabricated by a decal transfer method

Table 3
Comparison of different flow fields used in portable direct fuel cells

Flow field	Advantage	Disadvantages	Applications or study cases
Straight (parallel)	Lower pressure drops	Prone to inhomogeneous reactant distribution and product removal	Active DMFCs [14,31,32,35]
			Passive DMFC [48]
Serpentine (meander)	Helpful to remove gas product at the anode and water at the cathode, and to enhance two-phase mass transport	Higher pressure drops	Active DMFC [26,27,30,31]
		More parasitic energy required	
Spot (pin or grid)	Similar to straight flow fields as above	Similar to straight flow fields as above	Active DMFC [30]
Interdigitated	Enhanced local mass transport by both diffusion and forced convection	High-pressure difference required between channels High parasitic energy required	Active DMFC [28,30]
Porous media diffusion	Simple, low cost and compact	Lower mass transfer rates dependent on porous media Separate current collector needed	Passive DMFC [21,22,49]

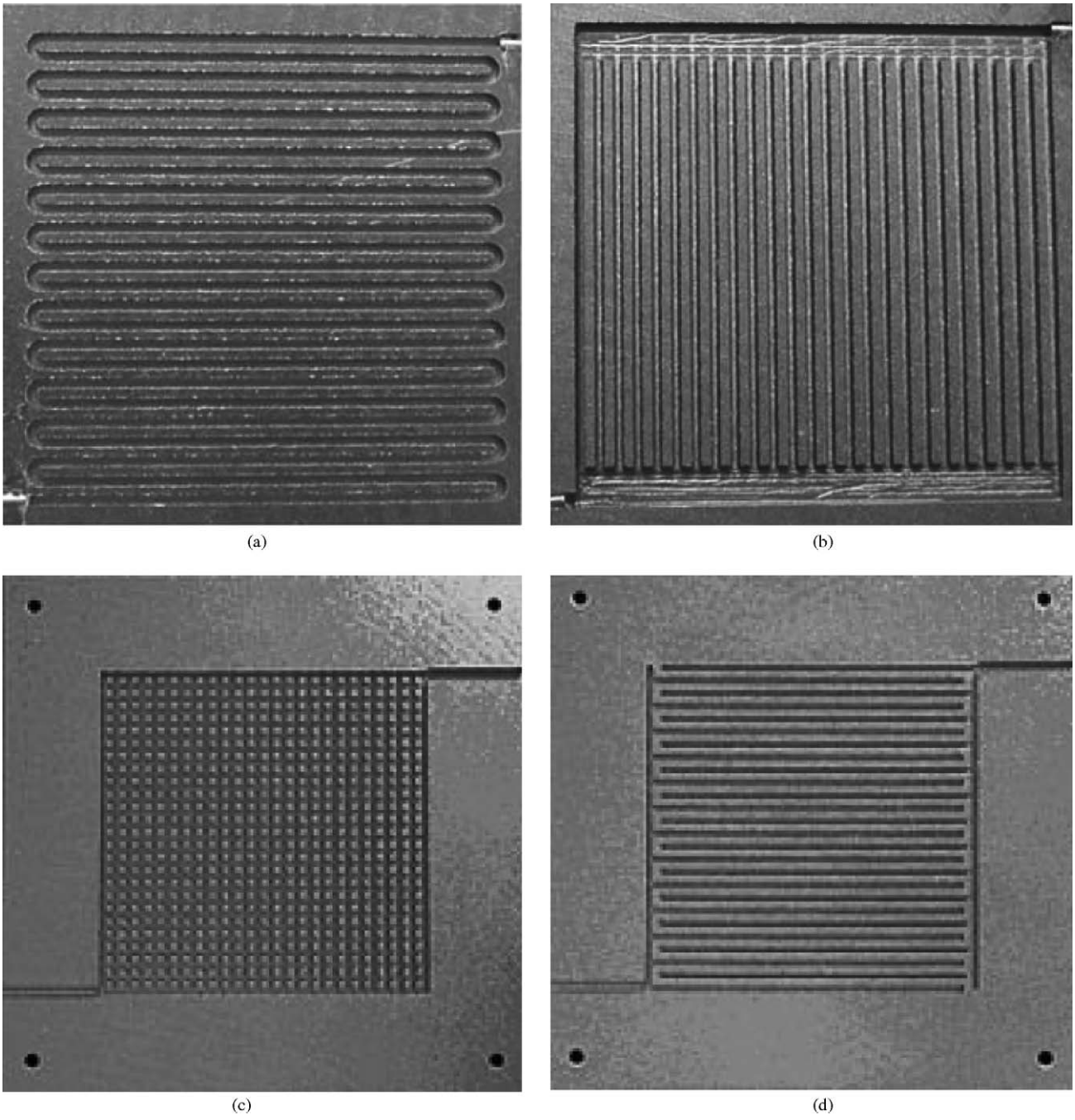

Fig. 7. Commonly used DFC flow fields: (a) serpentine; (b) straight [31], ©(2004), with permission from Elsevier; (c) spot; (d) interdigitated [30], ©(2004), with permission from John Wiley & Sons.

(DTM) and then used to form an MEA by sandwiching the CCM with off-the-shelf traditional anode and cathode backing layers [35].

2.4.2. Challenges for liquid fuel anodes

The liquid fuel anode in DFCs has to facilitate two-phase mass transfer, i.e. liquid fuel transport and gaseous product evolution transport. In general, hydrophilic micro-pores in the diffusion electrode are required to transport liquid fuels, and hydrophobic micro-pores are favourable to gas transport. Polytetrafluoroethylene (PTFE) and Nafion® are two commonly used polymeric additives used mainly as the bonding agent in PEM fuel cell electrodes. The presence of PTFE tends to make the electrode structure more hydrophobic. The influence of PTFE content in the DMFC anode has been investigated [34,36,37] and a PTFE content around 20 wt.% is generally found to be optimal. In contrast, Nafion® content makes the electrode more hydrophilic. Lindermeir et al. [33] implemented a hydrophilic modification using Nafion® ionomer as the binder compared with using PTFE at the equivalent amount (15 wt.%). The anodic diffusion layer then becomes more hydrophilic to facilitate methanol mass transport resulting in an increased DMFC

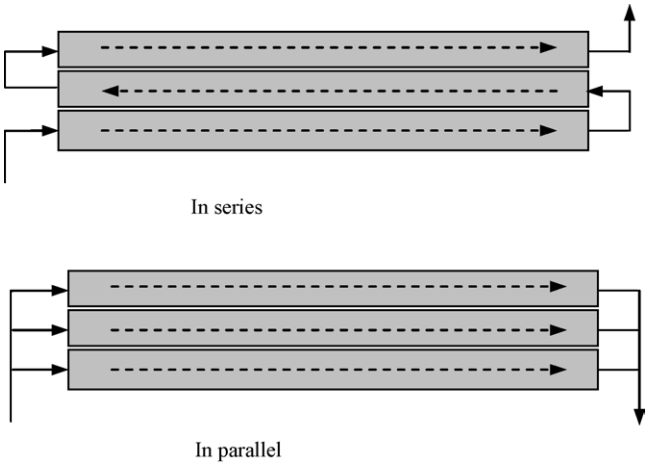

Fig. 8. Stack (three-cell) reactant feed configurations.

performance. Nafion® is also shown to help de-adsorb the CO on Pt–Ru catalysts in the methanol electro-oxidation process with an optimum composition in the range of 30–40 wt.% [38].

Some electrode treatment methods can be beneficial for the DFC anode. One treatment method is to electrochemically oxidize the carbonaceous electrode substrate in acidic solution before applying the electrocatalyst [39]. This treatment can make the substrate significantly more wettable improving liquid reactant distribution and catalyst penetration into the substrate. Another treatment method is to impregnate the treated (as above) substrate with a proton conducting ionomer before and after applying the electrocatalyst [40]. This is shown to improve performance again likely due to improved reactant distribution, increased proton conductivity, and increased catalyst distribution and utilization in the substrate.

Wilkinson et al. [41] proposed a multi-layer porous 3D electrode structure for direct liquid fuel cells to reduce fuel crossover and increase the fuel utilization. In one of the proposed configurations, as shown in Fig. 10, catalyst particles (86) are disposed at both major planar surfaces of each layer of porous electrically

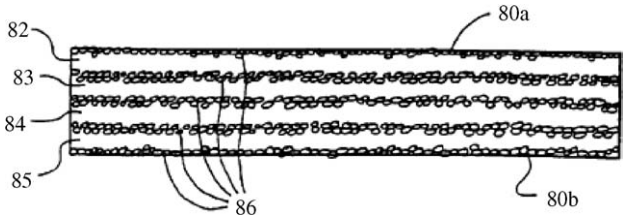

Fig. 10. A cross-section view of a multi-layer porous anode electrode, courtesy of [41].

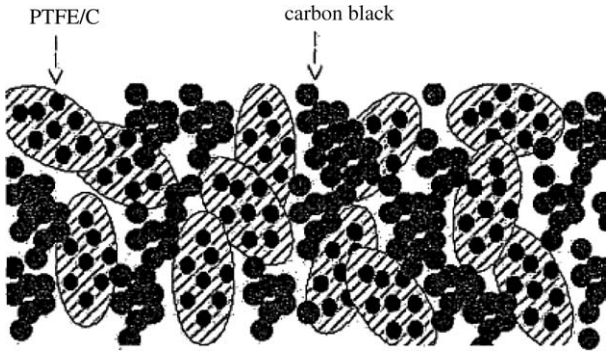

Fig. 11. A cross-section view of a diffusion electrode, courtesy of [42].

conductive sheet material, e.g. carbon fiber paper. Sufficient catalyst is provided so that substantially all of the methanol, which is introduced in a liquid to the electrode at surface (80a) is oxidized upon contacting surface (80b), which is adjacent to the membrane. The liquid fuel preferably contains acid to enhance the ionic conductivity in the electrode structure.

Kim and Choi [42] have proposed hydrophobic porous agglomerates (gas transporting path) and hydrophilic porous agglomerates (liquid and electron transporting path) continuously arranged through the thickness of the diffusion electrode including the catalyst layer, for both the anode and the cathode of the fuel cell, as shown in Fig. 11. When this duel-path microporous diffusion electrode structure is used in a DMFC,

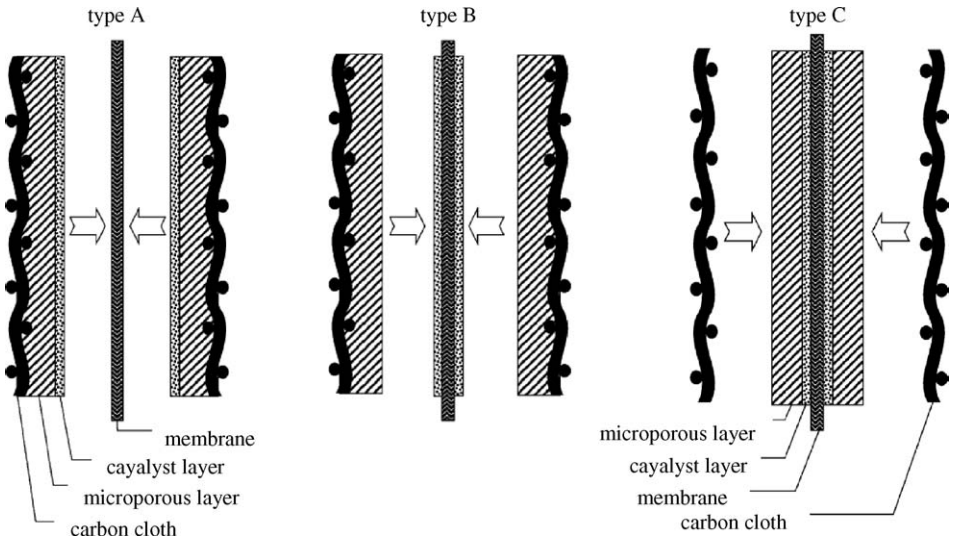

Fig. 9. MEA configurations [33], ©(2004), with permission from Elsevier.

for example the methanol solution can rapidly diffuse to the anode catalyst layer sites via the hydrophilic path in the diffusion layer and catalyst layer. The electrochemical reaction product gas (CO_2) can be easily discharged through the adjacent hydrophobic microporous path that remains open. Since the transport of aqueous methanol fuel and resulting gas product can rapidly pass through the separate paths, the electrochemical reaction at the catalyst sites can proceed rapidly with less mass transfer limitations and increased catalyst utilization.

Even with the hydrophilic micro-pores, it is still much harder for liquid fuels to get into the catalyst layer compared with gaseous fuels (e.g. H_2). Some researchers have dealt with this issue by adding a range of suitable proprietary pore-forming additives into the catalyst layer to increase the pore volume [43].

A novel three-dimensional electrode structure with large and small pores in the micrometer range is reported by Xie et al. [44]. The three-dimensional electrodes were prepared by initial synthesis of polystyrene spheres (PS) as structural building blocks. Different sizes of PS can be produced under particular conditions of the monomer concentration and temperature. Then PS spheres are coated with conducting polymers such as polypyrrole (Ppy). Finally, the catalyst is deposited on the surface of the conducting polymer network via an in situ reduction of precious metal salts. A SEM micrograph of the resulting electrode structure is shown in Fig. 12. Preliminary electrochemical characterization showed that the co-existence of large and small pores in the catalyst layer makes it easier for the transport of liquid fuels and also increases the active surface area for electrochemical reactions.

2.4.3. Challenges for passive air breathing DFCs

As previously mentioned, passive DFCs are more suitable for small portable power sources because of their compactness, potential for higher reliability, lower cost, higher fuel utilization and maximum energy density. However, without the use of external system devices for pumping liquid fuel and blowing air into the cells, passive DFCs have more challenges with respect to mass transport of reactants and products even at lower operating current densities. Cathode flooding is one of the major problems due to the decreased removal rate of excess water accumulated at the cathode from electro-osmotic drag, the oxygen reduction reaction and diffusion. The duel-path microporous diffusion electrode structure proposed by Kim and Choi [42] should also be an effective design for improving the cathode water management. Different types of electrode backing layers were reported to have a significant influence on the performance of a DMFC in an active supply mode [45]. These investigation results should be also useful for a passive air breathing fuel cell. Recent research on passive air breathing DFCs [21,22,46–51] have addressed some issues such as membrane permeability/thickness and pore size effect in the catalyst support materials. Thicker membranes and a higher concentration of fuels may result in such benefits as less fuel crossover, higher energy density, less sensitivity to feed concentration fluctuations, and faster transient response to load. In the small passive air breathing DMFC application mentioned earlier (refer to Fig. 2), a pure methanol fuel has been used. In this case, the water needed for the anode electrochemical reaction have to come from the cathode through back diffusion. This approach helps to reduce cathode flooding and results in a higher overall energy density. However, the issue of fuel crossover control becomes more challenging compared with the conventional approach of feeding the anode with a fuel/water mixture.

In general, MEA design for passive air breathing DFCs still requires significant improvements, particularly with respect to: (i) optimization of the three-dimensional anode to effectively increase power density and reduce fuel crossover especially for thinner membranes; (ii) more suitable cathode electrode structure to control the cathode flooding problem.

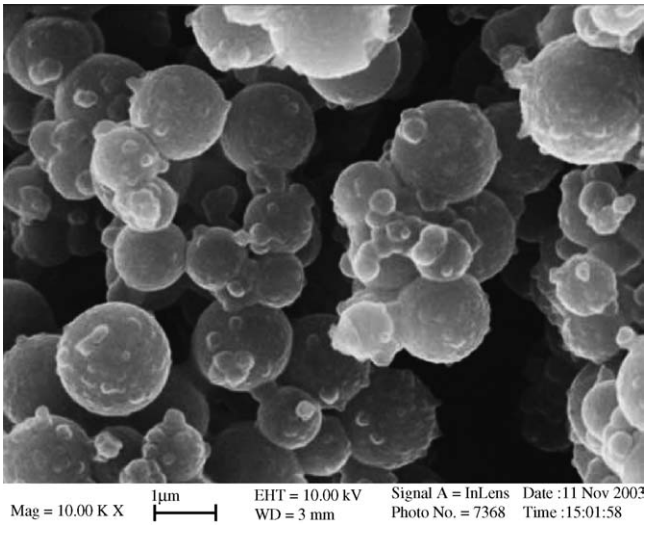

Fig. 12. A SEM micrograph of PS covered by Ppy [44], ©(2005), with permission from Elsevier.

3. Passive fuel distribution

Passive fuel distribution is desired for small and portable DFCs because it eliminates parasitic power consumption and results in a compact design with high energy density and efficiency. The simplest method for passive fuel distribution is to immerse the anode directly into a fuel reservoir, as shown in Fig. 5. However, this arrangement is not applicable to conventional bipolar flow field stacks. More effective passive fuel distribution designs are needed.

3.1. Passive natural-circulation fuel delivery

Based on the mechanism of traditional natural-circulation systems utilized in boilers, Ye and Zhao [52] have proposed a passive fuel delivery system for a DMFC, as shown in Fig. 13. The delivery system is driven by a density difference in the fuel flow loop as a result of the CO_2 gas bubbles generated. In general, this passive fuel delivery system was capable of achieving equivalent performance to a pump-fed cell, although some performance fluctuations at low current densities were reported. This performance fluctuation is primarily caused by fluctuations in the feed rate of the natural-circulation system because the CO_2 bubble generation rate is low at low current densities.

The most striking feature of this new fuel delivery system is that the fuel circulation flow rates increase with the operating

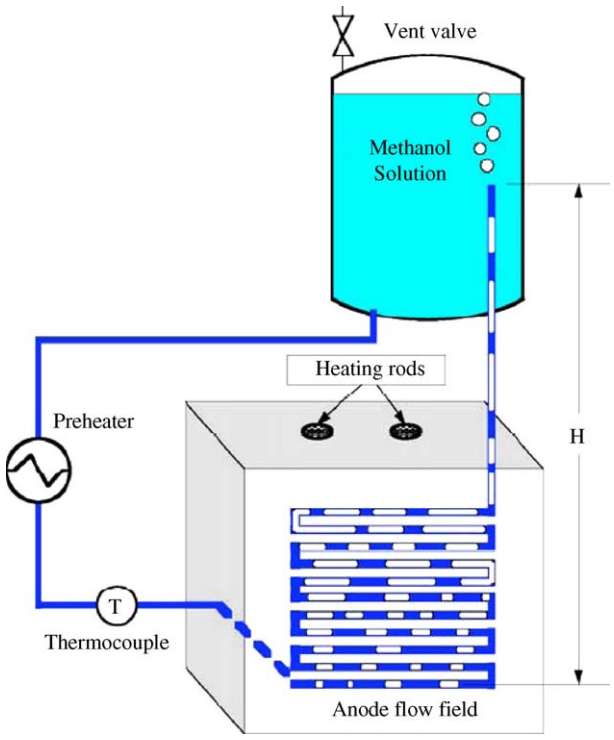

Fig. 13. A schematic natural-circulation in a DMFC cell [52], ©(2005), with permission from Elsevier.

electrical load and can be optimized for different operating conditions by selecting the right length and size of the inlet/outlet tubes, and fuel concentration. However, this type of fuel delivery system requires a minimum amount of vertical distance (*H*) between the fuel level in the tank and the bottom of the stack.

3.2. Passive fuel delivery with capillary flow

A method of transporting methanol into water through a wick material has been proposed by Guo and Cao [46]. They demonstrated that a wick material can be used to siphon neat methanol from one container into a separate container with dilute solution by capillary action. The wick can be a porous material such as ceramic, fiberglass, carbon fiber, polymers, or cotton. A fuel cell system with this passive fuel delivery mechanism is illustrated in Fig. 14.

A significant advantage of this capillary delivery system is that fuel and water can be carried separately and mixed in situ during fuel cell operation. Therefore, high energy density, high efficiency and reliability can be achieved by using this capillary delivery system in small portable DFCs.

3.3. Passive reactant delivery with self-pressurization

In order to enhance the effectiveness of passive fuel delivery methods by convective flow, capillary flow or natural diffusion, a reactant feed apparatus has been proposed by Zhang et al. [53]. As shown in Fig. 15, a pressurized anodic exhaust gas is utilized to drive liquid fuel into the anode and also drive oxidant/water in/out of the cathode (not shown in the schematic). The operation of this device requires a controlled three-way valve to direct the exhaust gas from the anode either to vent or to a self-pressurization chamber that is at one end of a cylinder. When the product gas line is switched to the vent, a pressure difference between the self-pressurization chamber and the released anode can drive liquid fuel stored at the other end of the cylinder via a piston into the anode compartment. This device has the advantages of a simple structure and negligible parasitic electrical power loss.

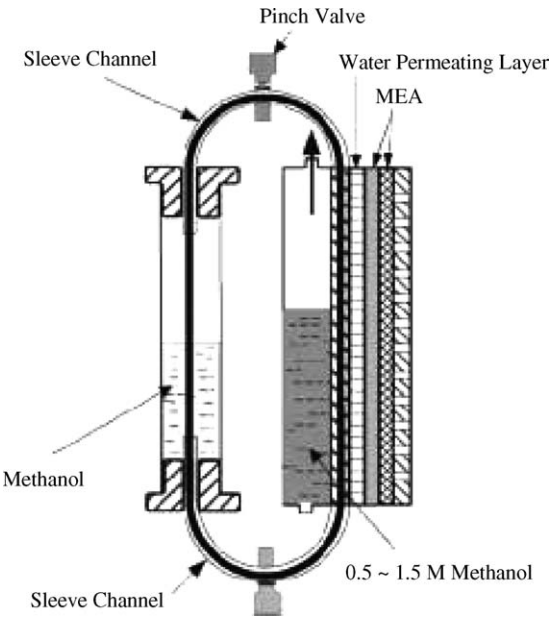

Fig. 14. A DMFC with a passive capillary methanol delivery system [46], ©(2004), with permission from Elsevier.

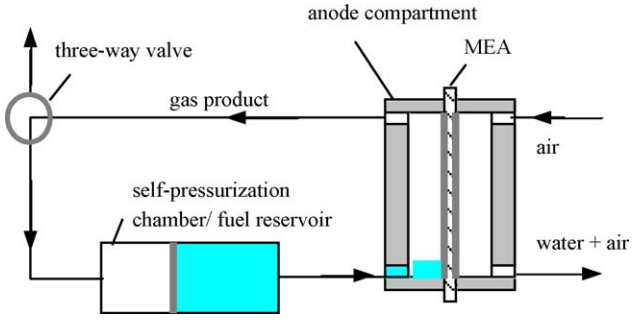

Fig. 15. A schematic for the passive reactant delivery system with self-pressurization.

4. Summary and conclusions

The liquid feed direct fuel cell (DFC) is an important portable power source moving into commercialization. The DFC cell, stack and system architecture is particularly important for portable applications where size and energy density are critical. Encouraging progress has been made with the DFC architecture with respect to stack and cell configuration, flow field design, MEA design, and methods of fuel delivery based on different system operating modes.

Active DFC systems can achieve higher current density and output power but often at the expense of greater system complexity and size, and lower energy density. This type of system is better for larger fuel cells. Passive DFC systems generally have less system complexity and size, and have the potential for higher reliability, lower cost, higher fuel utilization and energy density. This type of system is better suited to portable DFCs where the fuel cells are smaller. Passive DFC systems based on the bi-cell approach are more favorable for passive air breathing systems.

Many challenges exist for passive DFC systems that are air breathing and have a passive fuel delivery system. Further research and development in this area could significantly improve power and energy density, efficiency, cost and reliability for DFC portable applications.

References

[1] S. Song, W. Zhou, Z. Liang, R. Cai, G. Sun, Q. Xin, V. Stergiopoulos, P. Tsiakaras, Appl. Catal. B: Environ. 55 (2005) 65–72.
[2] Y.W. Rhee, S.Y. Ha, R.I. Masel, J. Power Sources 117 (2003) 35–38.
[3] Y. Zhu, Z. Khan, R.I. Masel, J. Power Sources 139 (2005) 15–20.
[4] Z. Qi, A. Kaufman, J. Power Sources 112 (2002) 121–129.
[5] D. Cao, S.H. Bergens, J. Power Sources 124 (2003) 12–17.
[6] J. Muller, P. Urban, R. Wezel, K.M. Colbow, J. Zhang, US Patent No. 6777116 (2004).
[7] E. Peled, T. Duvdevani, A. Aharon, A. Melman, Electrochem. Solid-State Lett. 4 (2001) A38–A41.
[8] K.M. Colbow, J. Zhang, K. Bai, US Patent Pub. No. 2004/0033397 (2004).
[9] S.R. Narayanan, E. Vamos, S. Surampudi, H. Frank, G. Halpert, G.K. Surya Prakash, M.C. Smart, R. Knieler, G.A. Olah, J. Kosek, C. Cropley, J. Electrochem. Soc. 144 (1997) 4195–4201.
[10] S. Surampudi, S.R. Narayanan, E. Vamos, H.A. Frank, G. Halpert, G.A. Olah, G.S. Prakash, US Patent No. 5599638 (1997).
[11] J. Zhang, K.M. Colbow, US Patent No. 6864001 (2005).
[12] K. Yamada, K. Asazawa, K. Yasuda, T. Ioroi, H. Tanaka, Y. Miyazaki, T. Kobayashi, J. Power Sources 115 (2003) 236–242.
[13] K. Yamada, K. Yasuda, H. Tanaka, Y. Miyazaki, T. Kobayashi, J. Power Sources 122 (2003) 132–137.
[14] C. Xie, J. Bostaph, J. Pavio, J. Power Sources 136 (2004) 55–65.
[15] G. McLean, Small Fuel Cells 2005, The Knowledge Foundation's Seventh Annual International Symposium, 27–29 April 2005, Washington, DC, USA.
[16] http://www.toshiba.co.jp/about/press/2004_06/pr2401.htm
[17] A.K. Shukla, P.A. Christensen, A. Hamnett, M.P. Hogarth, J. Power Sources 55 (1995) 87–91.
[18] M. Hogarth, P. Christensen, A. Hamnett, A. Shukla, J. Power Sources 69 (1997) 113–136.
[19] A. Heinzel, C. Hebling, M. Muller, M. Zedda, C. Muller, J. Power Sources 105 (2002) 250–255.
[20] R. Jiang, D. Chu, J. Power Sources 93 (2001) 25–31.
[21] T. Shimizu, T. Momma, M. Mohamedi, T. Osaka, S. Sarangapani, J. Power Sources 137 (2004) 277–283.
[22] D. Kim, E.A. Cho, S.A. Hong, I.H. Oh, H.Y. Ha, J. Power Sources 130 (2004) 172–177.
[23] D. Linden, US Patent No. 3718507 (1973).
[24] N.J. Fletcher, G.J. Lamont, V. Basura, H.H. Voss, D.P. Wilkinson, US Patent No. 5470671 (1995).
[25] D. Brett, N. Brandon, Fuel Cell Rev. February–March (2005).
[26] H. Yang, T.S. Zhao, Electrochim. Acta 50 (2005) 3243–3252.
[27] H. Yang, T.S. Zhao, Q. Ye, J. Power Sources 142 (2005) 117–124.
[28] A.S. Arico, P. Creti, V. Baglio, E. Modica, V. Antonucci, J. Power Sources 91 (2000) 202–209.
[29] X. Li, I. Sabir, Int. J. Hydrogen Energy 30 (2005) 359–371.
[30] A. Oedegaard, S. Hufschmidt, R. Wilmshoefer, C. Hebling, Fuel Cells 4 (2004) 219–224.
[31] K. Tuber, A. Oedegaard, M. Hermann, C. Hebling, J. Power Sources 131 (2004) 175–181.
[32] H. Dohle, T. Bewer, J. Mergel, R. Neitzel, D. Stolten, Fuel Cell Seminar October 30–November 2, 2000, Portland, Oregon, USA, 2000, pp. 130–133.
[33] A. Lindermeir, G. Rosenthal, U. Kunz, U. Hoffmann, J. Power Sources 129 (2004) 180–187.
[34] J. Nordlund, A. Roessler, G. Lindbergh, J. Appl. Electrochem. 32 (2002) 259–265.
[35] S.Q. Song, Z.X. Liang, W.J. Zhou, G.Q. Sun, Q. Xin, V. Stergiopoulos, P. Tsiakaras, J. Power Sources 145 (2005) 495–501.
[36] Z. Wei, S. Wang, B. Yi, J. Liu, L. Chen, W. Zhou, W. Li, Q. Xin, J. Power Sources 106 (2002) 364–369.
[37] V. Gogel, T. Frey, Z. Yongsheng, K.A. Friedrich, L. Jorissen, J. Garche, J. Power Sources 127 (2004) 172–180.
[38] Y.H. Chu, Y.G. Shul, W.C. Choi, S.I. Woo, H.S. Han, J. Power Sources 118 (2003) 334–341.
[39] K.M. Colbow, J. Zhang, D.P. Wilkinson, US Patent No. 6153323 (2000).
[40] J. Zhang, K.M. Colbow, D.P. Wilkinson, US Patent No. 6187467 (2001).
[41] D.P. Wilkinson, M.C. Johnson, K.M. Colbow, S.A. Campbell, US Patent No. 5874182 (1999) and US Patent No. 5672439 (1997).
[42] J. Kim, K. Choi, European Patent Application EP1519433A1 (2005).
[43] S. Gamburzev, A.J. Appleby, J. Power Sources 107 (2002) 5–12.
[44] F. Xie, Z. Tian, H. Meng, P.K. Shen, J. Power Sources 141 (2005) 211–215.
[45] A. Oedegaard, C. Hebling, A. Schmitz, S. Moller-Holst, R. Tunold, J. Power Sources 127 (2004) 187–196.
[46] Z. Guo, Y. Cao, J. Power Sources 132 (2004) 86–91.
[47] J. Han, E.S. Park, J. Power Sources 112 (2002) 477–483.
[48] J.G. Liu, T.S. Zhao, Z.X. Liang, R. Chen, J. Power Sources, in press.
[49] J.G. Liu, T.S. Zhao, R. Chen, C.W. Wong, Electrochem. Commun. 7 (2005) 288–294.
[50] G.G. Park, T.H. Yang, Y.G. Yoon, W.Y. Lee, C.S. Kim, Int. J. Hydrogen Energy 28 (2003) 645–650.
[51] C.Y. Chen, P. Yang, J. Power Sources 123 (2003) 37–42.
[52] Q. Ye, T.S. Zhao, J. Power Sources 147 (2005) 196–202.
[53] J. Zhang, K.M. Colbow, A.N.L. Lee, B. Lin, US Patent Pub. No. 20040131898 (2004).